

2000-0000
10-27-88
211722
A-10

**THE MODE III CRACK PROBLEM IN BONDED MATERIALS
WITH A NONHOMOGENEOUS INTERFACIAL ZONE**

by

F. Erdogan
A.C. Kaya
P.F. Joseph

Lehigh University
Bethlehem, PA 18015

October 1988

(NASA-CR-185315) THE MODE III CRACK PROBLEM
IN BONDED MATERIALS WITH A NONHOMOGENEOUS
INTERFACIAL ZONE (Lehigh Univ.) 33 p

N89-23927

CSCI 20K

Unclas
0211722

63/39

THE NATIONAL AERONAUTICS AND SPACE ADMINISTRATION
GRANT NAG-1-713

**THE MODE III CRACK PROBLEM IN BONDED MATERIALS
WITH A NONHOMOGENEOUS INTERFACIAL ZONE**

by

F. Erdogan

A.C. Kaya

P.F. Joseph

**Lehigh University
Bethlehem, PA 18015**

October 1988

**THE NATIONAL AERONAUTICS AND SPACE ADMINISTRATION
GRANT NAG-1-713**

THE MODE III CRACK PROBLEM IN BONDED MATERIALS WITH A NONHOMOGENEOUS INTERFACIAL ZONE

by

F. Erdogan, A.C. Kaya¹ and P.F. Joseph

Lehigh University, Bethlehem, PA 18015

Abstract

In this paper the mode III crack problem for two bonded homogeneous half planes is considered. The interfacial zone is modelled by a nonhomogeneous strip in such a way that the shear modulus is a continuous function throughout the composite medium and has discontinuous derivatives along the boundaries of the interfacial zone. The problem is formulated for cracks perpendicular to the nominal interface and is solved for various crack locations in and around the interfacial region. The asymptotic stress field near the tip of a crack terminating at an interface is examined and it is shown that, unlike the corresponding stress field in piecewise homogeneous materials, in this case the stresses have the standard square root singularity and their angular variation is identical to that of a crack in a homogeneous medium. With application to the subcritical crack growth process in mind, the results given include mostly the stress intensity factors for some typical crack geometries and various material combinations.

1. Introduction

In studying the fracture process in bonded materials, there are two groups of problems in which the mechanical modelling of interfacial regions may play a major role. The first is "debonding" and the second, crack penetration. The investigation of the debonding process requires the solution of a crack problem in which the crack is located in the interfacial zone and is parallel to the nominal interface. To study the second problem one may need the solution of a crack which lies in a plane generally perpendicular to the nominal interface and which intersects the interfacial region. Even though there are cases such as certain geophysical problems and some transient thermal stress problems involving materials with heavily temperature dependent material properties in which the constituent materials under consideration are inherently nonhomogeneous, in many engineering applications the logical assumption has been to treat the bonded materials as piecewise homogeneous media. Within

¹Assistant Professor, Department of the Mechanical Engineering, Middle East Technical University, Ankara, Turkey

the context of the linear elastic theory the only time such an idealized model of the interfacial regions leads to certain physical anomalies appears to be the presence of a crack in the medium that either lies along or intersects the interface.

As observed, for example, by Muskhelishvili (1953), Erdogan (1963,1965), England (1965), and Rice and Sih (1965), in the case of an interface crack the power of the crack tip singularity is complex predicting a physically unacceptable result, namely the interference of crack surface displacements (see also Comninou (1977) and Atkinson (1977) for further discussion of the problem based on the crack closure concept). For a crack intersecting the ideal bimaterial interface perpendicularly the physical difficulty arises from the fact that the analysis gives a singularity that is not the standard square root type. It was shown, for example, by Cook and Erdogan (1972) that for a crack terminating at a bimaterial interface, depending on the relative magnitudes of material constants, the power of stress singularity may be greater or less than 0.5. Similarly, Erdogan and Biricikoglu (1973) showed that for a crack crossing the interface the stress state exhibits a weak power singularity at the point of intersection (see also Bogy (1968,1971) and Hein and Erdogan (1971) for results in bonded wedges). The consequence of these analytical results is that in such problems, since the stresses and displacements near the crack tip do not remain self-similar as the crack propagates, it is not possible to calculate the strain energy release rate and to apply the techniques of the conventional fracture mechanics.

For a more accurate representation of the actual physical problem in bonded materials involving cracks it is clear that one needs to reexamine both the material model and the interface model. Maintaining the ideal interface model, Knowles and Sternberg (1975) and Shih and Asaro (1987) studied the interface crack problem for a nonlinear elastic material bonded to a rigid half space. Even though the anomalous deformation behavior at the crack tip may perhaps be rectified by a proper choice of the material model, it is highly unlikely that changes in material model alone will be sufficient to affect the standard square root singularity for a crack terminating at the interface and to eliminate the weak power singularity for a crack crossing the interface. This is then an important motivation to experiment with the mechanical modelling of interfacial zones. Another reason is, of course, the actual physical nature of interfacial zones. In many cases, regardless of the particular mechanism of the binding process, for thermodynamical consistency the interfacial region needs to be considered as a distinct phase (see, for example, the review article by Good (1967)). There is always some interdiffusion taking place across the interface so that there is usually a gradual change in the volume concentration of certain elements belonging to the adjacent material. Because of this even in diffusion bonding in which the thickness of the reaction zone may be only a few atomic layers, the actual thickness of the region having very steep variation in material properties may be substantially greater.

The basic assumption made in this study in modelling the interfacial zone, therefore, is that the mechanical properties of the composite medium may exhibit no jump discontinuities. The interfacial zone is thus assumed to be a thin elastic layer between two homogeneous materials with steeply varying mechanical properties. The corresponding plane elasticity problem for a crack lying in the nonhomogeneous interfacial region and parallel to the nominal interface was considered by Delale and Erdogan (1988a). The important special case of the "interface" crack in which the crack is located in the plane where the variation of the Young's modulus forms a kink was studied by Delale and Erdogan (1988b) who showed that by using this model the oscillatory behavior predicted by the ideal interface model does indeed disappear (see also Atkinson (1977) and Atkinson and List (1978) for related studies). The main interest in this study is in the crack penetration problem. To cover all possible crack configurations it is assumed that the medium contains three collinear cracks one in each constituent material oriented perpendicularly to the nominal interface. The medium is assumed to be under antiplane shear loading with displacements specified away from the crack region. The corresponding crack problem for two bonded nonhomogeneous half planes under mode III loading conditions was studied by Erdogan (1985). The important result found by Erdogan was that for the crack tip terminating at the kink plane of modulus distribution the stress state has the standard square root singularity.

2. Formulation of the Problem

Consider the antiplane shear problem shown in Fig. 1. Assume that the medium is loaded away from the crack region, the "homogeneous" problem in the absence of cracks has been solved, and

$$\sigma_{iyz}(x,0) = \tau_i(x) = -\sigma_{yz}^h(x,0), \quad a_i < x < b_i, \quad i=1,2,3 \quad (1)$$

are the only external forces. We further assume that, compared to the crack lengths and the layer thickness h , the thickness of the homogeneous materials 2 and 3 are large and hence can be treated as being infinite, and the shear modulus of the interfacial layer is given by

$$\mu_1(x) = \mu_2 e^{\beta x}, \quad 0 \leq x \leq h. \quad (2)$$

From (2) and $\mu_1(h) = \mu_3$ it follows that

$$\beta = \frac{1}{h} \log(\mu_3/\mu_2). \quad (3)$$

Noting that $y=0$ is a plane of symmetry, the problem shown in Fig. 1 may be formulated as

follows:

$$\nabla^2 w_1 + \beta \frac{\partial w_1}{\partial x} = 0, \quad 0 < x < h, \quad 0 \leq y < \infty, \quad (4)$$

$$\nabla^2 w_2 = 0, \quad -\infty < x < 0, \quad 0 \leq y < \infty, \quad (5)$$

$$\nabla^2 w_3 = 0, \quad h < x < \infty, \quad 0 \leq y < \infty, \quad (6)$$

$$w_1(0,y) = w_2(0,y), \quad \sigma_{1xz}(0,y) = \sigma_{2xz}(0,y), \quad 0 \leq y < \infty, \quad (7a,b)$$

$$w_1(h,y) = w_3(h,y), \quad \sigma_{1xz}(h,y) = \sigma_{3xz}(h,y), \quad 0 \leq y < \infty, \quad (8a,b)$$

$$w_1(x,0) = 0, \quad 0 < x < a_1, \quad b_1 < x < h, \quad (9a,b)$$

$$\sigma_{1yz}(x,0) = \tau_1(x), \quad a_1 < x < b_1,$$

$$w_2(x,0) = 0, \quad -\infty < x < a_2, \quad b_2 < x < 0, \quad (10a,b)$$

$$\sigma_{2yz}(x,0) = \tau_2(x), \quad a_2 < x < b_2,$$

$$w_3(x,0) = 0, \quad h < x < a_3, \quad b_3 < x < \infty \quad (11a,b)$$

$$\sigma_{3yz}(x,0) = \tau_3(x), \quad a_3 < x < b_3.$$

We now express the solution of (4)-(6) in the following form²:

$$w_j(x,y) = \frac{1}{2\pi} \int_{-\infty}^{\infty} f_j(y,\alpha) e^{-i\alpha x} d\alpha + \frac{2}{\pi} \int_0^{\infty} g_j(x,\alpha) \sin(y\alpha) d\alpha + c_j, \quad (j=1,2,3). \quad (12)$$

From (4)-(6) and (12) it may be shown that

²In (12) c_1, c_2, c_3 are included to account for possible rigid body displacements when the cracks cross the interfaces. If, however, in the analysis the continuity conditions (7a) and (8a) are replaced by

$$\frac{\partial}{\partial y} w_1(0,y) = \frac{\partial}{\partial y} w_2(0,y), \quad \frac{\partial}{\partial y} w_1(h,y) = \frac{\partial}{\partial y} w_3(h,y), \quad 0 \leq h < \infty, \quad (A)$$

these constants disappear and conditions (9a), (10a) and (11a) along with (A) insures the single-valuedness and continuity of the displacements.

$$f_1(y,\alpha) = A_1(\alpha)e^{m_1 y}, \quad y \geq 0, \quad (13)$$

$$g_1(x,\alpha) = B_1(\alpha)e^{n_1 x} + B_2(\alpha)e^{n_2 x}, \quad 0 < x < h, \quad (14)$$

$$f_2(y,\alpha) = A_2(\alpha)e^{-|\alpha|y}, \quad y \geq 0, \quad (15)$$

$$g_2(x,\alpha) = D(\alpha)e^{\alpha x}, \quad x < 0, \quad (16)$$

$$f_3(y,\alpha) = A_3(\alpha)e^{-|\alpha|y}, \quad y \geq 0, \quad (17)$$

$$g_3(x,\alpha) = C(\alpha)e^{-\alpha x}, \quad x > 0 \quad (18)$$

where

$$m_1 = -|\alpha|\sqrt{1 + \frac{i\beta}{\alpha}}, \quad (19)$$

$$n_1 = -\frac{\beta}{2} + \alpha_1, \quad n_2 = -\frac{\beta}{2} - \alpha_1, \quad \alpha_1 = \alpha\sqrt{1 + \left(\frac{\beta}{2\alpha}\right)^2}. \quad (20)$$

Introducing the unknown functions

$$\phi_j(x) = \frac{\partial}{\partial x} w_j(x,0), \quad a_j < x < b_j, \quad j=1,2,3, \quad (21)$$

from (12)-(19) and (21) we obtain

$$A_j(\alpha) = \frac{i}{\alpha} \int_{a_j}^{b_j} \phi_j(t)e^{i\alpha t} dt. \quad (22)$$

It should be observed that at $y=\mp 0$ the solution must satisfy the following conditions (Fig. 1):

$$\lim_{y \rightarrow +0} w_2(x,y) = 0, \quad x < a_2,$$

$$\lim_{y \rightarrow +0} w_2(0,y) = \lim_{y \rightarrow +0} w_1(0,y),$$

$$\lim_{y \rightarrow +0} w_1(h,y) = \lim_{y \rightarrow +0} w_3(h,y),$$

$$\lim_{y \rightarrow +0} w_3(x,y) = 0, \quad x > b_3. \quad (23a-d)$$

By substituting from (12)-(18) and (22) into (23a-c) we find

$$c_2 = \frac{1}{2} \int_{a_2}^{b_2} \phi_2(t) dt ,$$

$$c_1 - c_2 = \frac{1}{2} \int_{a_1}^{b_1} \phi_1(t) dt + \frac{1}{2} \int_{a_2}^{b_2} \phi_2(t) dt ,$$

$$c_3 - c_1 = \frac{1}{2} \int_{a_1}^{b_1} \phi_1(t) dt + \frac{1}{2} \int_{a_3}^{b_3} \phi_3(t) dt , \quad (24a-c)$$

which determine the constants c_1 , c_2 and c_3 . The fourth condition in (23) gives

$$c_3 = -\frac{1}{2} \int_{a_3}^{b_3} \phi_3(t) dt \quad (25)$$

which, with (24), implies that

$$\sum_{j=1}^3 \int_{a_j}^{b_j} \phi_j(t) dt = 0 . \quad (26)$$

Note that if the cracks are disconnected (9a), (10a) and (11a) require ϕ_j defined by (21) to satisfy the following conditions:

$$\int_{a_j}^{b_j} \phi_j(t) dt = 0 , \quad j=1,2,3. \quad (27)$$

From (24) and (27) it is seen that in this case the constants c_j would be zero. However, if two or all three cracks are connected, then the appropriate combination of (26) and (27) provide the single-valuedness conditions and (24) gives c_1 , c_2 and c_3 .

If we now substitute from (12)-(18) into the homogeneous conditions (7) and (8), observe that

$$\sigma_{jxy} = \mu_j \frac{\partial w_j}{\partial x} , \quad \sigma_{jyz} = \mu_j \frac{\partial w_j}{\partial x} , \quad j=1,2,3 , \quad (28)$$

invert the sine transforms, we obtain

$$B_1(\alpha) + B_2(\alpha) - D(\alpha) = R_1(\alpha) ,$$

$$n_1 B_1(\alpha) + n_2 B_2(\alpha) - \alpha D(\alpha) = R_2(\alpha) ,$$

$$e^{n_1 h} B_1(\alpha) + e^{n_2 h} B_2(\alpha) - e^{-\alpha h} C(\alpha) = R_3(\alpha) ,$$

$$n_1 e^{n_1 h} B_1(\alpha) + n_2 e^{n_2 h} B_2(\alpha) + \alpha e^{-\alpha h} C(\alpha) = R_4(\alpha), \quad (29a-d)$$

where the functions R_i , ($i=1, \dots, 4$) are given in Appendix A. Thus, from (29) and (A6) it follows that

$$\begin{aligned} B_1(\alpha) &= \frac{1}{\Delta} \left\{ \frac{\alpha(\alpha+n_2)}{2\alpha_1} \int_{a_1}^{b_1} \left[\frac{(\alpha-n_1)}{n_1} e^{-2\alpha_1 h} e^{-n_1 t} + \frac{(\alpha-n_2)}{n_2} e^{-n_1 h} e^{n_2(h-t)} \right] \phi_1(t) dt \right. \\ &\quad \left. - (\alpha+n_2) \int_{a_2}^{b_2} e^{-2\alpha_1 h} e^{\alpha t} \phi_2(t) dt - (\alpha-n_2) \int_{a_3}^{b_3} e^{-n_1 h} e^{-\alpha(t-h)} \phi_3(t) dt \right\}, \\ B_2(\alpha) &= \frac{1}{\Delta} \left\{ \frac{\alpha(\alpha-n_1)}{2\alpha_1} \int_{a_1}^{b_1} \left[\frac{(\alpha+n_1)}{n_1} e^{-n_1 t} - \frac{(\alpha+n_2)}{n_2} e^{-n_1 h} e^{n_2(h-t)} \right] \phi_1(t) dt \right. \\ &\quad \left. + (\alpha+n_1) \int_{a_2}^{b_2} e^{\alpha t} \phi_2(t) dt + (\alpha-n_1) \int_{a_3}^{b_3} e^{-n_1 h} e^{-\alpha(t-h)} \phi_3(t) dt \right\}, \\ C(\alpha) &= \frac{e^{\alpha h}}{\Delta} \left\{ \int_{a_1}^{b_1} \left[\frac{\alpha(\alpha-n_1)}{n_1} e^{n_2 h} e^{-n_1 t} - \frac{\alpha(\alpha-n_2)}{n_2} e^{n_2(h-t)} \right] \phi_1(t) dt \right. \\ &\quad \left. + 2\alpha_1 \int_{a_2}^{b_2} e^{n_2 h} e^{\alpha t} \phi_2(t) dt - \frac{\beta}{2} \int_{a_3}^{b_3} (1 - e^{-2\alpha_1 h}) e^{-\alpha(t-h)} \phi_3(t) dt \right\}, \\ D(\alpha) &= \frac{1}{\Delta} \left\{ \int_{a_1}^{b_1} \left[\frac{\alpha(\alpha+n_1)}{n_1} e^{-n_1 t} + \frac{\alpha(\alpha+n_2)}{n_2} e^{-n_1 h} e^{n_2(h-t)} \right] \phi_1(t) dt \right. \\ &\quad \left. - \frac{\beta}{2} \int_{a_2}^{b_2} (1 - e^{-2\alpha_1 h}) e^{\alpha t} \phi_2(t) dt - 2\alpha_1 \int_{a_3}^{b_3} e^{-n_1 h} e^{-\alpha(t-h)} \phi_3(t) dt \right\}, \end{aligned} \quad (30a-d)$$

where

$$\Delta = (\alpha-n_1)(\alpha+n_2)e^{-2\alpha_1 h} - (\alpha+n_1)(\alpha-n_2). \quad (31)$$

3. The Integral Equations

In the previous section the problem has been formulated in terms of three unknown functions ϕ_1 , ϕ_2 and ϕ_3 . These functions are determined by using (9b), (10b) and (11b) which

are the only conditions that have not yet been satisfied. Thus, by substituting (12)-(18) and (28) into (9b), (10b) and (11b) we obtain

$$\begin{aligned}
\lim_{y \rightarrow +0} \sigma_{1yz}(x,y) &= \frac{\mu_1(x)}{2\pi} \lim_{y \rightarrow +0} \int_{-\infty}^{\infty} m_1 A_1(\alpha) e^{m_1 y - i\alpha x} d\alpha \\
&+ \frac{2\mu_1(x)}{\pi} \int_0^{\infty} [B_1(\alpha) e^{n_1 x} + B_2(\alpha) e^{n_2 x}] \alpha d\alpha = \tau_1(x), \quad a_1 < x < b_1, \\
\lim_{y \rightarrow +0} \sigma_{2yz}(x,y) &= \frac{\mu_2}{2\pi} \lim_{y \rightarrow +0} \int_{-\infty}^{\infty} -|\alpha| A_2(\alpha) e^{-|\alpha| y - i\alpha x} d\alpha \\
&+ \frac{2\mu_2}{\pi} \int_0^{\infty} \alpha D(\alpha) e^{\alpha x} d\alpha = \tau_2(x), \quad a_2 < x < b_2, \\
\lim_{y \rightarrow +0} \sigma_{3yz}(x,y) &= \frac{\mu_3}{2\pi} \lim_{y \rightarrow +0} \int_{-\infty}^{\infty} -|\alpha| A_3(\alpha) e^{-|\alpha| y - i\alpha x} d\alpha \\
&+ \frac{2\mu_3}{\pi} \int_0^{\infty} \alpha C(\alpha) e^{-\alpha x} d\alpha = \tau_3(x), \quad a_3 < x < b_3. \tag{32a-c}
\end{aligned}$$

By substituting from (22) and (30) into (32) we obtain the following system of integral equations for ϕ_j , ($j=1,2,3$):

$$\lim_{y \rightarrow +0} \sum_{j=1}^3 \int_{a_j}^{b_j} h_{ij}(x,y,t) \phi_j(t) dt = \frac{\pi}{\mu_i} \tau_i(x), \quad a_i < x < b_i. \tag{33}$$

The singular parts of the kernels in (33) can be separated after performing the appropriate asymptotic analysis. Note that the leading terms in the asymptotic expansion of the infinite intergrals giving the kernels in (33) are identical to that given by Erdogan (1985). Therefore, the details of the analysis will not be given in this paper. Thus, by following the procedure described by Erdogan (1985) (33) may be reduced to

$$\int_{a_j}^{b_j} \sum_{i=1}^3 [\frac{\delta_{ij}}{t-x} + k_{ij}(x,t)] \phi_j(t) dt = \frac{\pi}{\mu_j} \tau_j(x), \quad a_i < x < b_i \tag{34}$$

where the kernels k_{ij} , ($i,j=1,2,3$) are given in Appendix B.

In examining the asymptotic behavior of the kernels for cracks fully embedded in the three materials shown in Fig. 1, that is for $b_2 < 0$, $a_1 > 0$, $b_1 < h$ and $a_3 > h$, it is sufficient to

separate the singular parts of the kernels that become unbounded for $x=t$ only. However, if one or two crack tips touch one of the interfaces $x=0$ or $x=h$, then it is necessary to separate, in addition to the parts that are singular at $x=t$, the terms that become unbounded at $x=t=0$, ($a_2 < (t,x) < b_1$) and at $x=t=h$, ($a_1 < (t,x) < b_3$). The inspection of the kernels given in (34) and Appendix B shows that for embedded cracks as expected the only unbounded terms in the kernels that may influence the nature of the crack tip singularity are $(t-x)^{-1}$. The remaining unbounded terms are logarithmic (i.e., $\log|t-x|$) which are square integrable and may be treated as Fredholm kernels. It is also seen that the terms that become unbounded for $x=t=0$ and $x=t=h$ are $\log|t+x|$ and $\log|2h-x-t|$. Again, these terms would have no influence on the crack tip singularity. One may, therefore, conclude that in this problem for all crack geometries the displacement derivative at the crack tip would have the standard square root singularity. Also, as in the case of piecewise homogeneous materials considered by Erdogan and Cook (1974), there would be no singularity at the point of intersection of the crack and the interface.

4. Stress Distribution Near the Crack Tips and Stress Intensity Factors

The stress distribution near the crack tips may be obtained by examining the asymptotic behavior of the corresponding expressions found by substituting from (12)-(18) and (30) into (28) for small values of r , where r is the radial distance from the crack tips. Consider, for example, the distribution of σ_{1yz} around an embedded crack in material 1. From (32a) and (22) the leading term for σ_{1yz} may be expressed as

$$\sigma_{1yz}(x,y) \cong \frac{\mu_1(x)}{2\pi} \int_{a_1}^{b_1} \phi_1(t) dt \int_{-\infty}^{\infty} \frac{im_1}{\alpha} e^{m_1 y} e^{i\alpha(t-x)} d\alpha. \quad (35)$$

Also, from (34) it is clear that the solution of the singular integral equations is of the form

$$\phi_j(t) = \frac{G_j(t)}{\sqrt{(t-a_j)(b_j-t)}}, \quad a_j < t < b_j. \quad (36)$$

Thus, observing that for $|\alpha| \rightarrow \infty$ $m_1 \cong -|\alpha|$ and defining

$$t = \frac{b_1-a_1}{2} \tau + \frac{b_1+a_1}{2}, \quad x = \frac{b_1-a_1}{2} \xi + \frac{b_1+a_1}{2}, \quad y = \frac{b_1-a_1}{2} \eta, \\ \alpha = \frac{2}{b_1-a_1} s, \quad G_1(t) = F_1(\tau), \quad (37)$$

(35) becomes

$$\sigma_{1yz}(x,y) \doteq \frac{i\mu_1(x)}{\pi(b_1-a_1)} \int_{-\infty}^{\infty} \frac{|s|}{s} e^{-|s|\eta-is\xi} ds \int_{-1}^1 \frac{F_1(\tau)}{\sqrt{1-\tau^2}} e^{is\tau} d\tau. \quad (38)$$

Again, since the possible unbounded terms in (38) are determined by the leading terms in the integrand for $s \rightarrow \infty$, by using (see, for example, Gradshteyn and Ryzhik, (1965))

$$\int_{-1}^1 \frac{F_1(\tau)}{\sqrt{1-\tau^2}} e^{is\tau} d\tau = \sqrt{\frac{\pi}{2|s|}} [F_1(1)e^{i(s-\frac{\pi|s|}{4s})} + F_1(-1)e^{-i(s-\frac{\pi|s|}{4s})}] + O(\frac{1}{s}), \quad (39)$$

we find

$$\sigma_{1yz}(x,y) \doteq \frac{2\mu_1(x)}{\pi(b_1-a_1)} \sqrt{\frac{\pi}{2}} \int_0^{\infty} \frac{e^{-\eta s}}{\sqrt{s}} \{-F_1(1)\sin[(\xi-1)s+\frac{\pi}{4}] - F_1(-1)\sin[(\xi+1)s-\frac{\pi}{4}]\} ds. \quad (40)$$

Similarly from (see Gradshteyn and Ryzhik, (1965))

$$\int_0^{\infty} s^{\mu-1} e^{-\eta s} \left\{ \frac{\sin cs}{\cos cs} \right\} ds = \frac{\Gamma(\mu)}{(\eta^2+c^2)^{\mu/2}} \left\{ \frac{\sin}{\cos} \right\} (\mu \tan^{-1} \frac{c}{\eta}) \quad (41)$$

and (40) it may easily be shown that

$$\sigma_{1yz}(x,y) \doteq -\frac{\mu_1(x)}{(b_1-a_1)/2} \frac{F_1(1)}{\sqrt{2\rho}} \cos \frac{\theta}{2} + \frac{\mu_1(x)}{(b_1-a_1)/2} \frac{F_1(-1)}{\sqrt{2\rho}} \sin \frac{\theta}{2}, \quad (42)$$

where

$$\rho \cos \theta = \xi-1, \quad \rho \sin \theta = \eta \quad \text{and} \quad \rho \cos \theta = \xi+1, \quad \rho \sin \theta = \eta \quad (43)$$

near $\xi=1$ and $\xi=-1$, respectively. If we now use (37), from (42) we obtain

$$\sigma_{1yz}(x,y) \doteq -\frac{\mu_1(b_1)}{\sqrt{(b_1-a_1)/2}} \frac{G_1(b_1)}{\sqrt{2r}} e^{\beta r \cos \theta} \cos \frac{\theta}{2}, \quad r \cos \theta = x-b_1, \quad r \sin \theta = y \quad (44)$$

near $x=b_1, y=0$ and

$$\sigma_{1yz}(x,y) \doteq \frac{\mu_1(a_1)}{\sqrt{(b_1-a_1)/2}} \frac{G_1(a_1)}{\sqrt{2r}} e^{\beta r \cos \theta} \sin \frac{\theta}{2}, \quad r \cos \theta = x-a_1, \quad r \sin \theta = y, \quad (45)$$

near $x=a_1, y=0$.

Based on the asymptotic results expressed in (44) and (45) one may observe that

(a) If we define the mode III stress intensity factors

$$k_3(a_1) = \lim_{x \rightarrow a_1} \sqrt{2(a_1-x)} \sigma_{1yz}(x,0), \quad k_3(b_1) = \lim_{x \rightarrow b_1} \sqrt{2(x-b_1)} \sigma_{1yz}(x,0), \quad (46)$$

from (44) and (45) it is seen that

$$k_3(a_1) = \frac{\mu_1(a_1)}{\sqrt{(b_1-a_1)/2}} G_1(a_1), \quad k_3(b_1) = -\frac{\mu_1(b_1)}{\sqrt{(b_1-a_1)/2}} G_1(b_1). \quad (47a,b)$$

These results are identical to that found for homogeneous materials.

(b) Note that since expression (32a) for σ_{1yz} is valid for $0 < x < h$ and since the form of the solution given by (36) for $\phi_1(t)$ remains unchanged for $a_1=0$ and $b_1=h$, the expressions giving the stress distribution around the crack tips would remain valid for the limiting cases $a_1=0$ and $b_1=h$ provided θ is restricted to $0 < \theta < \pi/2$ for $a_1=0$ in (45) and $\pi/2 < \theta < \pi$ for $b_1=h$ in (44).

(c) Expressions similar to (44) and (45) can easily be developed for $\sigma_{1xz}(x,y)$ near the crack tips. It can indeed be shown that the expressions for σ_{1xz} are identical to (44) and (45) provided $\cos(\theta/2)$ is replaced by $\sin(\theta/2)$ in (44) and $\sin(\theta/2)$ by $\cos(\theta/2)$ in (45).

(d) Aside from the factor $e^{\beta r \cos \theta}$, the stress distributions (44) and (45) are identical to that found for homogeneous materials. However, note that the expressions are valid only for "small" values of r for which $e^{\beta r \cos \theta}$ is nearly unity.

(e) From the foregoing results it does not automatically follow that for the limiting cases $a_1=0$ and $b_1=h$ (Fig. 1) (47) is still valid and the validity of the expressions (44) and (45) can be extended into materials 3 and 2, respectively. To examine this problem we now consider the distribution of $\sigma_{2yz}(x,y)$ near the crack tip $(a_1,0)$ for the limiting case of $a_1=0$ $b_2 < 0$. Following Erdogan (1985), the leading term for σ_{2yz} may be expressed as³

$$\sigma_{2yz}(x,y) \doteq \frac{\mu_2 e^{\gamma x}}{\pi} \int_0^{b_1} \phi_1(t) e^{(\beta t - \gamma x)/2} dt \int_0^\infty e^{-\alpha(t-x)} \cos \alpha y d\alpha. \quad (48)$$

By using the definitions (37) (with $F_1(\tau) = G_1(t) e^{\beta t/2}$) from (48) we find

$$\sigma_{2yz}(x,y) \doteq \frac{2\mu_2 e^{\gamma x/2}}{\pi b_1} \int_0^\infty e^{s\xi} \cos \eta s ds \int_{-1}^1 \frac{F_1(\tau)}{\sqrt{1-\tau^2}} e^{-s\tau} d\tau. \quad (49)$$

³In Erdogan (1985) μ_2 as well as μ_1 is a function of x ($\mu_2 e^{\gamma x}$ and $\mu_2 e^{\beta x}$, respectively). Thus, by assuming that both β and γ are nonzero, the asymptotic results given here cover all limiting crack geometries that may arise from Fig. 1.

If we define

$$F_1(\tau) = \sum_0^{\infty} A_n T_n(\tau), \quad (T_n(\tau) = \cos n\theta_0, \quad \tau = \cos\theta_0) \quad (50)$$

and use (see Erdelyi (1953))

$$\int_0^{\pi} e^{-s \cos\theta_0} \cos n\theta_0 d\theta_0 = (-1)^n \pi I_n(s) \quad (51)$$

(49) becomes

$$\sigma_{2yz}(x,y) \doteq \frac{2\mu_2 e^{\gamma x/2}}{b_1} \sum_0^{\infty} (-1)^n A_n \int_0^{\infty} e^{s\xi} I_n(s) \cos\eta s ds \quad (52)$$

where T_n is the Chebyshev polynomial and I_n is the modified Bessel function. Now by observing that

$$T_n(s) \doteq \frac{e^s}{\sqrt{2\pi s}} \quad \text{for } s \rightarrow \infty \quad \text{and} \quad \sum_0^{\infty} (-1)^n A_n = F_1(-1), \quad (53)$$

from (37), (52) and (53) we find

$$\sigma_{2yz}(x,y) = \frac{\mu_2}{\sqrt{b_1}} e^{\gamma x/2} F_1(-1) \int_0^{\infty} \frac{1}{\sqrt{\alpha}} e^{\alpha x} \cos\alpha y d\alpha. \quad (54)$$

In material 2 near the crack tip ($a_1=0, y=0$) we have

$$x < 0, \quad -x = r \cos\theta_1, \quad y = r \sin\theta_1, \quad (55)$$

where θ_1 is measured from the negative x axis. Thus from (54), (41), (55) and $F_1(-1)=G_1(0)$ it may be shown that

$$\sigma_{2yz}(x,y) \doteq \frac{\mu_2 e^{-\frac{1}{2}\gamma r \cos\theta_1}}{\sqrt{b_1}} \frac{G_1(r \cos\theta_1) e^{\frac{1}{2}\beta r \cos\theta_1}}{\sqrt{2r}} \cos \frac{\theta_1}{2}. \quad (56)$$

If we define the stress intensity factor at the crack tip ($a_1=0, y=0$) by

$$k_3(0) = \lim_{x \rightarrow -0} \sqrt{-2x} \sigma_{2yz}(x,0) \quad (57)$$

from (56) and (55) it is seen that

$$k_3(0) = \frac{\mu_2}{\sqrt{b_1}} G_1(0), \quad (58)$$

which is identical to (47a) with $a_1=0$. Since $\theta_1=\pi-\theta$, also note that aside from the factors $\exp(\beta r \cos\theta)$, $\exp(\frac{1}{2}\beta r \cos\theta_1)$ and $\exp(-\frac{1}{2}\beta r \cos\theta_1)$ the stress distributions (45) and (56) are identical. From a practical viewpoint since all asymptotic expressions such as (56) are valid only for $r \rightarrow 0$, in (44), (45) and (56) all factors involving e^r should be ignored. This leads to a very simple and important conclusion, namely that the behavior of the singular field near the crack tip in nonhomogeneous materials is identical to that in homogeneous materials provided $\mu(x,y)$ is a continuous (but not necessarily a differentiable) function.

5. The Solution and Results

By defining the normalized quantities

$$t = \frac{b_j - a_j}{2} r + \frac{b_j + a_j}{2}, \quad x = \frac{b_j - a_j}{2} s + \frac{b_j + a_j}{2}, \quad \phi_j(t) = f_j(r),$$

$$\frac{b_j - a_j}{2} k_{ij}(x,t) = K_{ij}(r,s), \quad \frac{\pi}{\mu_i(x)} \tau_i(x) = g_i(s), \quad (i,j=1,2,3), \quad (59)$$

for disconnected cracks the integral equations (34) and conditions (27) may be expressed as

$$\int_{-1}^1 \sum_1^3 \left[\frac{\delta_{ij}}{r-s} + K_{ij}(s,r) \right] f_j(r) dr = g_i(s), \quad -1 < x < 1, \quad (i=1,2,3), \quad (60)$$

$$\int_{-1}^1 f_j(r) dr = 0, \quad (j=1,2,3). \quad (61)$$

Equations (60) are solved by letting

$$f_j(r) = \frac{F_j(r)}{\sqrt{1-r^2}}, \quad F_j(r) = \sum_0^{N_j} c_{jn} T_n(r) \quad (62)$$

and by using

$$\int_{-1}^1 \frac{T_n(r) dr}{(r-s)\sqrt{1-r^2}} = \pi U_{n-1}(s), \quad (n \geq 1), \quad |s| < 1, \quad (63)$$

$$\int_{-1}^1 \frac{T_n(r)}{\sqrt{1-r^2}} \log|r-s| dr = -\frac{\pi}{n} T_n(s), \quad (n \geq 1), \quad |s| < 1 \quad (64)$$

to regularize the system. From (62), (61) and the orthogonality of $T_n(r)$ it may be shown that $c_{j0}=0$, ($j=1,2,3$). The functional equations resulting from (60) and (62)-(64) may be solved by "collocation". Thus, by specifying s (60) and (61) may be reduced to the following algebraic system:

$$\sum_{j=1}^3 \sum_{n=1}^{N_j} c_{jn} H_{ijn}(s_{im}) = g_i(s_{im}), \quad (i=1,2,3; m=1,2,\dots,N_j). \quad (65)$$

In (65) rapidly converging results are obtained by selecting s_{im} as the roots of the Chebyshev polynomials $T_{N_j}(s)$ as follows:

$$s_{im} = \cos\left(\frac{2m-1}{2N_j} \pi\right), \quad (i=1,2,3; m=1,\dots,N_j). \quad (66)$$

After solving the integral equations, the stress intensity factors defined by (46) and (47) may be obtained as

$$k_3(a_j) = \lim_{x \rightarrow a_j} \mu_j(x) \sqrt{2(x-a_j)} \phi_j(x) = \mu_j(a_j) \sqrt{\frac{b_j-a_j}{2}} F_j(-1),$$

$$k_3(b_j) = -\lim_{x \rightarrow b_j} \mu_j(x) \sqrt{2(b_j-x)} \phi_j(x) = -\mu_j(b_j) \sqrt{\frac{b_j-a_j}{2}} F_j(1), \quad (j=1,2,3). \quad (67a,b)$$

Also, from (21), (59) and (62) the crack surface displacements are found to be

$$w_i(x,+0) = \int_{a_i}^x \phi_i(x) dx = -\frac{b_i-a_i}{2} \sum_{n=1}^{N_i} \frac{1}{n} c_{in} U_{n-1}(s) \sqrt{1-s^2},$$

$$s = \frac{2}{b_i-a_i} \left(x - \frac{b_i+a_i}{2}\right), \quad (i=1,2,3). \quad (68)$$

The results given by (59)-(68) are valid for all disconnected crack geometries, including the cracks terminating at "interfaces" $x=0$ and $x=h$. For cracks crossing the interfaces, since the intersection point of the crack and the interface is not a singular point, the problem can be solved by treating the connected crack as a single crack. For example, if the medium contains

a single crack along $y=0$, $a_2 < x < b_1$ (34) and (27) may be replaced by

$$\int_{a_2}^{b_1} k(x,t)\phi(t)dt = \pi\tau(x), \quad a_2 < x < b_1, \quad (69)$$

$$\int_{a_2}^{b_1} \phi(t)dt = 0, \quad (70)$$

where

$$\phi(t) = \begin{cases} \phi_2(t), & a_2 < t \leq 0, \\ \phi_1(t), & 0 \leq t < b_1, \end{cases} \quad (71)$$

$$\tau(x) = \begin{cases} \tau_2(x)/\mu_2, & a_2 < x \leq 0, \\ \tau_1(x)/\mu_1(x), & 0 \leq x < b_1, \end{cases} \quad (72)$$

$$k(x,t) = \frac{1}{t-x} + k_{22}(x,t), \quad a_2 < x \leq 0, \quad a_2 < t \leq 0,$$

$$k(x,t) = k_{21}(x,t), \quad a_2 < x \leq 0, \quad 0 \leq t < b_1,$$

$$k(x,t) = k_{12}(x,t), \quad 0 \leq x < b_1, \quad a_2 < t \leq 0, \quad (73)$$

$$k(x,t) = \frac{1}{t-x} + k_{11}(x,t), \quad 0 \leq x < b_1, \quad 0 \leq t < b_1.$$

The problem may then be solved by following the numerical technique described by (59)-(68). Specifically, by selecting $\phi(t)=f(r)$, $a_2 < t < b_1$, $-1 < r < 1$, as in (62), the stress intensity factors and the crack opening displacement may be obtained from (67) and (68).

Some calculated results are shown in Tables 1-5 and Figures 2 and 3. From the geometry of the medium it is clear that an external load giving rise to only σ_{xz} in the crack region would have no effect on the crack problem; that is, for this case the relative crack surface displacements and the stress intensity factors would be zero. In the problem under consideration from a practical viewpoint perhaps the most important external load would, therefore, be a uniform shear strain $\gamma_{yz}=\gamma_0$ applied to the composite medium away from the

crack region. Thus, the perturbation problem will be solved under the following crack surface tractions:

$$\tau_i(x) = -\sigma_{yz}^h(x,0) = -\gamma_0\mu_i(x), \quad a_i < x < b_i, \quad (i=1,2,3). \quad (74)$$

Table 1 shows the stress intensity factors for two different material pairs containing a single crack in either material 2 or material 3. In both cases one crack tip is assumed to touch the interface $x=0$ or $x=h$. The table shows the normalized stress intensity factor defined by

$$k(d_i) = k_3(d_i)/\tau_0\sqrt{a}, \quad \tau_0 = \mu_2\gamma_0 \quad (75)$$

where $2a$ is the crack length and d_i designates the crack tip. For $h/a \rightarrow 0$, as expected, the stress intensity factors approach the corresponding homogeneous results, namely

$$k_3(a_i) \rightarrow k_3(b_i) \rightarrow \mu_i\gamma_0\sqrt{a}, \quad (i=2,3), \quad (76)$$

where $a_2 = -2a$, $b_2 = 0$, $a_3 = h$, $b_3 = 2a$. For $h/a \rightarrow 0$ one would expect to recover the solution of the corresponding crack problem in a piecewise homogeneous material (see Erdogan and Cook (1974)). In this case near the crack tip terminating at the interface the stress state has the behavior $\sigma_{iz} \sim r^{-\alpha}$, ($i=x,y$), where r is the distance from the crack tip. Since $\mu_2 > \mu_3$, $\alpha > 0.5$ for the crack in material 2 and $\alpha < 0.5$ for the crack in material 3. In the limit as $h/a \rightarrow 0$, therefore, $k(0) \rightarrow \infty$ and $k(h) \rightarrow 0$. The stress intensity factors at the far ends of the cracks shown in the table are obtained by using the solution given by Erdogan and Cook (1974). For $\mu_2 = 4\mu_3$ results showing the trends for small values of h/a are also displayed in Fig. 2.

For a crack in material 1 with the crack tip at $b_1 = h$ and having a length of $2a < h$ or $2a > h$, the stress intensity factors are given in Table 2. The results for the similar problem with a crack tip at $x=0$ are shown in Table 3. Again, it is expected that for $h/a \rightarrow 0$ $k_3(d_i) \rightarrow \mu_i(d_i)\gamma_0\sqrt{a}$. Observing that k_3 is normalized with respect to $\mu_2\gamma_0\sqrt{a}$, this is seen to be the trend in Tables 2 and 3. For $h/a \rightarrow 0$ the stress intensity factors are seen to approach the limiting values given in Table 1 for the piecewise homogeneous material.

In applications the results given in Table 1 would correspond to a subcritically propagating crack one end of which is arrested by a relatively tough interfacial zone. If the interfacial zone is less resistant to crack growth than the adjacent materials, then the crack is more likely to initiate in the interfacial zone, propagate through, become arrested by the tougher of the two materials, and grow into the other. Such a process may be studied by using the results similar to that given by Tables 2 and 3.

The stress intensity factors for a crack of length $2a$ centered at $x=h/2$ with $2a \lesseqgtr h$ are

given in Table 4. Note that for $a/h \rightarrow 0$, as expected, we have

$$k_3(a_1) \rightarrow k_3(b_1) \rightarrow \mu_1(h/2)\gamma_0\sqrt{a}, \quad (77)$$

that is, $k \rightarrow 0.5$ for $\mu_2/\mu_3=4$ and $k \rightarrow 0.1$ for $\mu_2/\mu_3=100$. Similarly, for $a/h \rightarrow \infty$ the stress intensity factors at the crack tips approach the corresponding homogeneous half plane solutions⁴. For a crack embedded in material 2 or material 3 some results are given in Table 5. In order to compare the results found in this paper with the limiting results obtained by Erdogan and Cook (1974) and by Kaya and Erdogan (1987), in Table 5 μ_2/μ_3 is assumed to be 23.08 (roughly corresponding to an aluminum-epoxy pair).

Finally, Fig. 3 shows some sample results for the crack opening displacement $w(s)=w(x,0)$ where s is the normalized coordinate defined by (59) with $s=\mp 1$ corresponding to the crack tips. Three examples shown correspond to $h/a=0, 0.25$ and 1 , $2a$ being the crack length. In each case the centerline of the interfacial zone coincides with the quarter point of the crack, and the boundaries of the interfacial zone are indicated by solid vertical lines. For $h=0$ as shown by Erdogan and Cook (1974) the function $\phi(x) = (\partial/\partial x)w(x,0)$ is discontinuous at the interface. This may also be seen in Fig. 3. $w(x)$, however, becomes progressively smoother for increasing values of h/a .

Acknowledgement. This study was supported by NSF under the grant MSM-8613611, by NASA-Langley under the grant NAG-1-713 and by SRC Contract 88-MP-071.

References

1. Atkinson, C., 1977, "On Stress Singularities and Interfaces in Linear Elastic Fracture Mechanics", International Journal of Fracture, Vol. 13, pp. 807-820.
2. Atkinson, C. and List, R.D., 1978, "Steady State Crack Propagation into Media with Spatially Varying Elastic Properties", Int. J. Engng. Sci., Vol. 16, pp. 717-730.
3. Bogy, D.B., 1968, "Edge-Bonded Dissimilar Orthogonal Elastic Wedges Under Normal and Shear Loading", ASME Journal of Applied Mechanis, Vol. 35, pp. 460-466.

⁴Note that for a homogeneous half plane with a stress-free boundary containing an edge crack of length a perpendicular to the boundary and subjected to uniform antiplane shear traction τ_0 on the crack surfaces, the stress intensity factor is $\tau_0\sqrt{a}$. In a piecewise homogeneous medium (i.e., for $h=0$) under uniform antiplane shear strain $\gamma_{yz}=\gamma_0$ away from the crack region, since for a symmetrically located crack ($-a < x < a$) $\sigma_{xy}(0,y)$ along the y axis is zero, the solution would be identical to that of two half planes with stress-free boundaries having edge cracks of length a (see Erdogan and Cook (1974)).

4. Bogy, D.B., 1971, "Two Edge-Bonded Elastic Wedges of Different Materials and Wedge Angles under Surface Traction", ASME Journal of Applied Mechanics, Vol. 38, pp. 377-386.
5. Comninou, M., 1977, "The Interface Crack", ASME Journal of Applied Mechanics, Vol. 44, pp. 631-636.
6. Cook, T.S. and Erdogan, F., 1972, "Stresses in Bonded Materials with a Crack Perpendicular to the Interface", Int. J. Engng. Sci., Vol. 10, pp. 677-697.
7. Delale, F. and Erdogan, F., 1988a, "On the Mechanical Modelling of the Interfacial Region in Bonded Half Planes", ASME Journal of Applied Mechanics, Vol. 55, pp. 317-324.
8. Delale, F. and Erdogan, F., 1988b, "Interface Crack in a Nonhomogeneous Elastic Medium", Int. J. Engng. Sci., Vol. 26, pp. 559-568.
9. England, A.H., 1965, "A Crack Between Dissimilar Media", ASME Journal of Applied Mechanics, Vol. 32, pp. 400-402.
10. Erdelyi, A. (ed.), 1953, Higher Transcendental Functions, Vol. II, McGraw-Hill Book Company, Inc., New York.
11. Erdogan, F., 1963, "Stress Distribution in a Nonhomogeneous Plane with Cracks", ASME Journal of Applied Mechanics, Vol. 3, pp. 232-236.
12. Erdogan, F., 1965, "Stress Distribution in Bonded Dissimilar Materials with Cracks", ASME Journal of Applied Mechanics, Vol. 32, pp. 403-410.
13. Erdogan, F. and Biricikoglu, V., 1973, "Two Bonded Half Planes with a Crack Going Through the Interface", Int. J. Engng. Sci., Vol. 11, pp. 745-766.
14. Erdogan, F. and Cook, T.S., 1974, "Antiplane Shear Crack Terminating at and Going Through a Bimaterial Interface", International Journal of Fracture, Vol. 10, pp. 227-240.
15. Erdogan, F., 1985, "The Crack Problem for Bonded Nonhomogeneous Materials Under Antiplane Shear Loading", ASME Journal of Applied Mechanics, Vol. 52, pp. 823-828.
16. Hein, V.L. and Erdogan, F., 1971, "Stress Singularities in a Two-Material Wedge", International Journal of Fracture, Vol. 7, pp. 317-330.
17. Gradshteyn, I.S. and Ryzhik, 1965, Tables of Integrals, Series and Products, Academic Press, New York.
18. Knowles, J.K. and Sternberg, E., 1975, "On the Singularity Induced by Certain Mixed Boundary Conditions in Linearized and Nonlinear Elastostatics", Int. J. Solids Structures, Vol. 11, pp. 1173-1201.
19. Muskhelishvili, N.I., 1953, Some Basic Problems of the Mathematical Theory of Elasticity, P. Noordhoff Ltd. Groningen-Holland.
20. Rice, J.R., and Sih, G.C., 1965, "Plane Problems of Cracks in Dissimilar Media", ASME

Journal of Applied Mechanics, Vol. 32, pp. 418-423.

21. Shih, C.F. and Asaro, R.J., 1987, "Elastic-Plastic Analysis of Cracks on Bimaterial Interfaces, Part I: Small Scale Yielding", Brown University Report ONR-N00014-86K-0235/2.

Table 1. Normalized mode 3 stress intensity factors for a crack of length $2a$ located in either material 2 or in material 3 with the inner crack tip touching its respective interface: $\mu_2/\mu_3 = 4, 100$, $k = k_3/\tau_0\sqrt{a}$, $\tau_0 = \gamma_0\mu_2$, γ_0 is uniform shear strain at $y \rightarrow \infty$.

$\mu_2/\mu_3 = 4$				
$2a/h$	crack in mat. 2		crack in mat. 3	
	$k(-2a)$	$k(0)$	$k(h)$	$k(2a+h)$
0.2	1.0070	1.017	.246	.2483
0.5	1.0153	1.039	.241	.2464
1.0	1.0254	1.071	.234	.2441
2.0	1.0385	1.125	.223	.2415
3.0	1.0471	1.169	.215	.2400
4.0	1.0532	1.206	.209	.2389
5.0	1.0579	1.239	.203	.2382
10.0	1.0716	1.364	.186	.2363
20.0	1.0831	1.524	.167	.2351
50.0	1.0945	1.79	.143	.2341
100.0	1.1005	2.04	.126	.2338
200.0	1.1049	2.34	.110	.2336
2000.0	1.112	4.	.06	.2334
$\rightarrow \infty$	1.1144	∞	0	.2333

$\mu_2/\mu_3 = 100$				
$2a/h$	crack in mat. 2		crack in mat. 3	
	$k(-2a)$	$k(0)$	$k(h)$	$k(2a+h)$
.2	1.021	1.053	.00951	.00980
.5	1.042	1.120	.00896	.00963
1.0	1.065	1.214	.00831	.00947
2.0	1.092	1.362	.00747	.00932
4.0	1.121	1.584	.00651	.00920
10.0	1.156	2.021	.00521	.00910
100.0	1.221	4.3	.00256	.00903
$\rightarrow \infty$	1.331	∞	0	.00902

Table 2. Normalized mode 3 stress intensity factors for a crack of length $2a$ with the right crack tip touching the 1-3 interface and the left crack tip either in material 1 ($2a/h \leq 1$) or in material 2 ($2a/h > 1$): $\mu_2/\mu_3 = 4, 100$, $k = k_3/\tau_0 \sqrt{a}$, $\tau_0 = \gamma_0 \mu_2$, γ_0 is uniform shear strain at $y \rightarrow \infty$.

$2a/h$	$\mu_2/\mu_3 = 4$		$\mu_2/\mu_3 = 100$	
	$k(h-2a)$	$k(h)$	$k(h-2a)$	$k(h)$
.2	.316	.254	.0216	.0105
.4	.399	.258	.0469	.0108
.6	.506	.262	.1034	.0110
.8	.647	.267	.234	.0112
1.0	.859	.275	.590	.0116
1.2	.963	.288	.816	.0131
1.5	1.028	.310	.966	.0158
2.0	1.077	.343	1.092	.0202
3.0	1.115	.395	1.202	.0279
5.0	1.135	.466	1.282	.0397
10.0	1.141	.568	1.336	.0598
20.0	1.138	.679	1.361	.0866

Table 3. Normalized mode 3 stress intensity factors for a crack of length $2a$ with the left crack tip touching the 2-1 interface and the right crack tip either in material 1 ($2a/h \leq 1$) or in material 3 ($2a/h > 1$): $\mu_2/\mu_3 = 4, 100$, $k = k_3/\tau_0 \sqrt{a}$, $\tau_0 = \gamma_0 \mu_2$, γ_0 is uniform shear strain at $y \rightarrow \infty$.

$2a/h$	$\mu_2/\mu_3 = 4$		$\mu_2/\mu_3 = 100$	
	$k(0)$	$k(2a)$	$k(0)$	$k(2a)$
.2	.980	.788	.919	.445
.4	.955	.617	.820	.188
.6	.926	.480	.728	.0774
.8	.894	.369	.651	.0312
1.0	.859	.275	.590	.01163
1.2	.821	.246	.541	.00865
1.5	.773	.233	.486	.00792
2.0	.712	.227	.423	.00783
3.0	.635	.225	.347	.00806
5.0	.551	.226	.271	.00838
10.0	.460	.229	.194	.00868
20.0	0	.233	0	.00901

Table 4. Normalized mode 3 stress intensity factors for a crack of length $2a$ centered at $h/2$ in material 1. Crack is either entirely in material 1 ($2a/h \leq 1$) or crosses both interfaces ($2a/h > 1$): $\mu_2/\mu_3 = 4, 100$, $k = k_3/\tau_0\sqrt{a}$, $\tau_0 = \gamma_0\mu_2$, γ_0 is uniform shear strain at $y \rightarrow \infty$.

2a/h	$\mu_2/\mu_3 = 4$		$\mu_2/\mu_3 = 100$	
	k(h/2-a)	k(h/2+a)	k(h/2-a)	k(h/2+a)
.2	.553	.449	.138	.0685
.4	.611	.401	.189	.0454
.6	.676	.357	.263	.0296
.8	.753	.316	.379	.0190
1.0	.859	.275	.590	.01163
1.4	.927	.255	.758	.00938
2.0	.956	.2493	.842	.00913
3.0	.973	.2477	.899	.00926
5.0	.985	.2478	.941	.00950
9.0	.992	.2485	.968	.00970
20.0	.996	.2492	.985	.00986
200.0	.9997	.2499	.999	.00999
$\rightarrow \infty$	1.0000	.2500	1.000	.01000

Table 5. Normalized mode 3 stress intensity factors for a crack of length $2a$ located in either material 2 or in material 3. The crack orientation with respect to its respective interface is constant and the position of the other interface is varied by changing $2a/h$: $\mu_2/\mu_3=23.08$, $k=k_3/\tau_0\sqrt{a}$, $\tau_0=\gamma_0\mu_2$, γ_0 is uniform shear strain at $y\rightarrow\infty$.

Crack in material 2						
$\frac{-(b_2+a_2)}{b_2-a_2}$	1.00		1.15		2.00	
$2a/h$	$k(a_2)$	$k(b_2)$	$k(a_2)$	$k(b_2)$	$k(a_2)$	$k(b_2)$
1.	1.0505	1.154	1.0390	1.0869	1.0159	1.0244
2.	1.0742	1.267	1.0541	1.0869	1.0196	1.0314
5.	1.1081	1.507	1.0717	1.2023	1.0228	1.0379
10.	1.1324	1.777	1.0810	1.2470	1.0241	1.0406
20.	1.1539	2.143	1.0868	1.2791	1.0248	1.0422
50.	1.177	2.81	1.0909	1.3034	1.0253	1.0432
100.	1.192	3.5	1.0923	1.3125	1.0254	1.0435
1000.			1.0937	1.3213	1.0255	1.0438
$\rightarrow\infty$	1.2558	∞	1.0938	1.3223	1.0256	1.0438

Crack in material 3						
$\frac{b_3+a_3-2h}{b_3-a_3}$	1.00		1.15		2.00	
$2a/h$	$k(a_3)$	$k(b_3)$	$k(a_3)$	$k(b_3)$	$k(a_3)$	$k(b_3)$
1.	0.0377	.04146	.03997	.04182	.04231	.04266
2.	0.0346	.04080	.03843	.04133	.04203	.04252
5.	0.0295	.04009	.03640	.04084	.04178	.04239
10.	0.0253	.03975	.03520	.04061	.04167	.04235
20.	0.0213	.03953	.03439	.04047	.04161	.04232
50.	0.0165	.03939	.03380	.04039	.04158	.04230
100.	0.0134	.03934	.03359	.04036	.04156	.04230
1000.		.03929	.03338	.04033	.04155	.04229
$\rightarrow\infty$	0	.03929	.03336	.04033	.04155	.04229

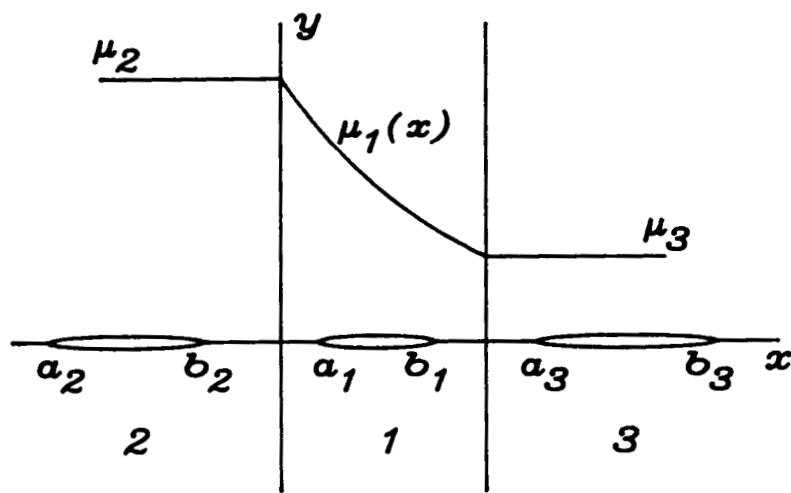


Fig. 1 Geometry of bonded materials containing cracks perpendicular to the nominal interface

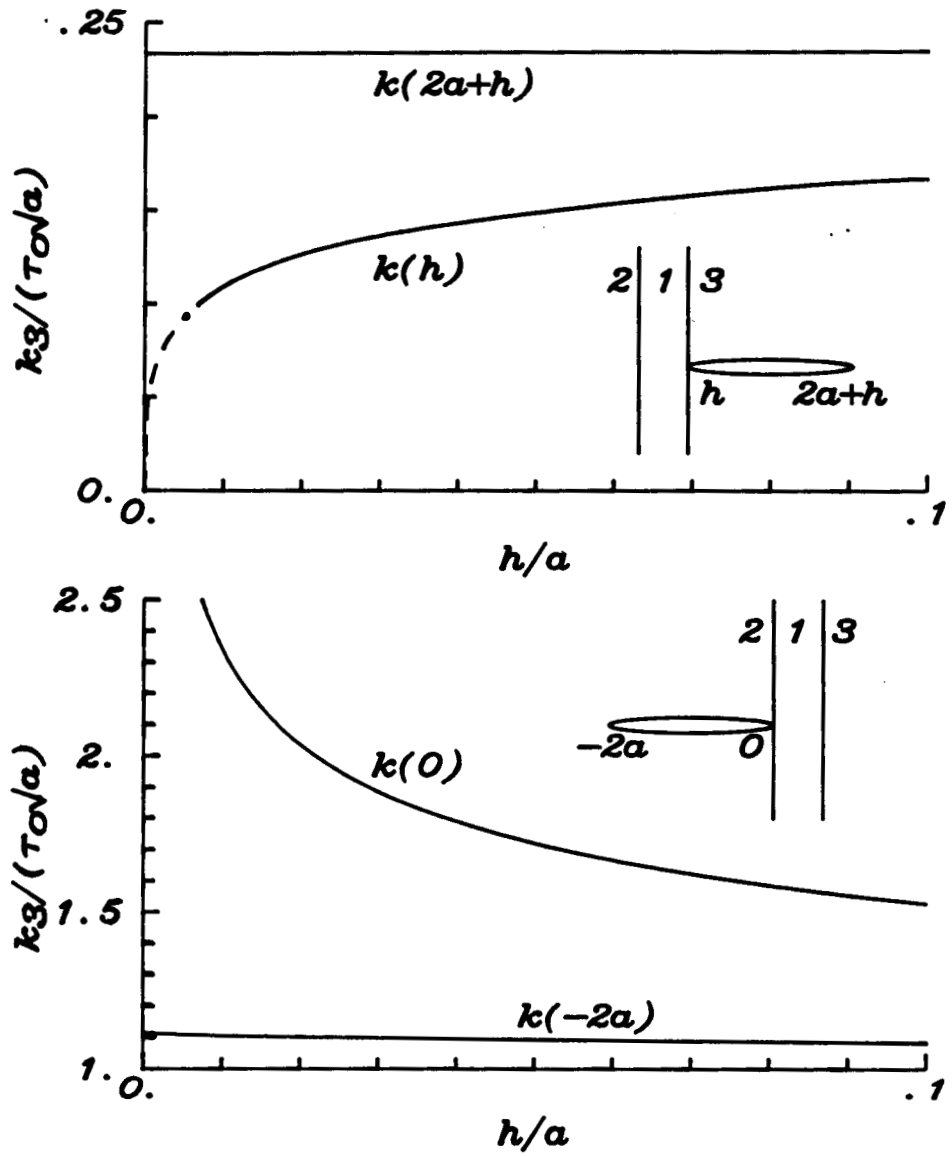


Fig. 2 Normalized stress intensity factors for the crack terminating at the interfacial zone in bonded materials; $\mu_2=4\mu_3$, $\tau_0=\mu_2\gamma_0$, where γ_0 is the uniform shear γ_{yz}^∞ away from the crack region.

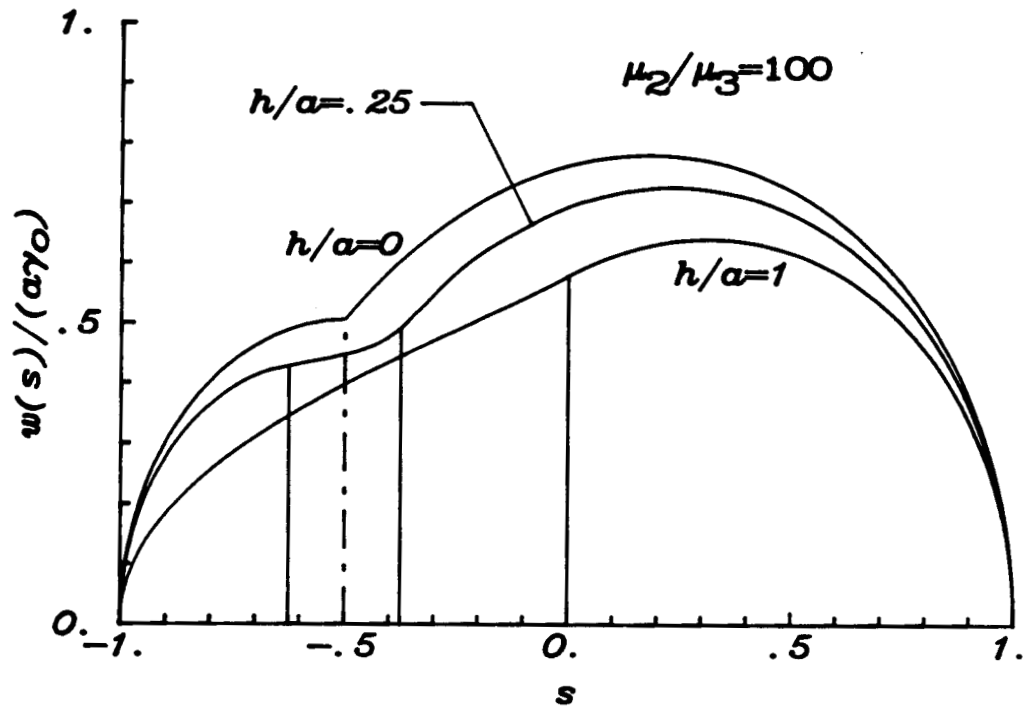


Fig. 3 Normalized crack surface displacement in bonded materials with a nonhomogeneous interfacial zone. In each case shown the crack goes through the zone and the centerline of the zone coincides with the quarter-point of the crack, $s = -0.5$, where s is the normalized coordinate defined by $x = s(b_3 - a_2)/2 + (b_3 + a_2)/2$ (Fig. 1).

APPENDIX A

Derivation of $R_1(\alpha), \dots, R_4(\alpha)$ that appear in (29)

Substituting from (12)-(18) and (28) into (7) and (8), inverting the sine transforms, changing the order of integrations, and evaluating the inner integrals, R_1, \dots, R_4 defined by (29) may be expressed as

$$\begin{aligned}
 R_1(\alpha) &= -\frac{1}{2\pi} \int_{-\infty}^{\infty} \frac{\alpha A_1(\theta) d\theta}{\alpha^2 + \theta^2 + i\beta\theta} + \frac{1}{2\pi} \int_{-\infty}^{\infty} \frac{\alpha A_2(\theta) d\theta}{\alpha^2 + \theta^2} + (c_2 - c_1) \frac{1}{\alpha}, \\
 R_2(\alpha) &= \frac{i}{2\pi} \int_{-\infty}^{\infty} \frac{\alpha \theta A_1(\theta) d\theta}{\alpha^2 + \theta^2 + i\beta\theta} - \frac{i}{2\pi} \int_{-\infty}^{\infty} \frac{\alpha \theta A_2(\theta) d\theta}{\alpha^2 + \theta^2}, \\
 R_3(\alpha) &= -\frac{1}{2\pi} \int_{-\infty}^{\infty} \frac{\alpha A_1(\theta) e^{-i\theta h} d\theta}{\alpha^2 + \theta^2 + i\beta\theta} + \frac{1}{2\pi} \int_{-\infty}^{\infty} \frac{\alpha A_3(\theta) e^{-i\theta h} d\theta}{\alpha^2 + \theta^2} + (c_3 - c_1) \frac{1}{\alpha}, \\
 R_4(\alpha) &= \frac{i}{2\pi} \int_{-\infty}^{\infty} \frac{\alpha \theta A_1(\theta) e^{-i\theta h} d\theta}{\alpha^2 + \theta^2 + i\beta\theta} - \frac{i}{2\pi} \int_{-\infty}^{\infty} \frac{\alpha \theta A_3(\theta) e^{-i\theta h} d\theta}{\alpha^2 + \theta^2}. \tag{A1-4}
 \end{aligned}$$

We now substitute from (22) into (A1-4), change the order of integrations, and evaluate the inner integrals by using the following results:

$$\int_{-\infty}^{\infty} \frac{e^{i\theta t}}{\alpha^2 + \theta^2} d\theta = \frac{\pi}{\alpha} e^{\alpha t}, \quad t < 0,$$

$$\int_{-\infty}^{\infty} \frac{e^{i\theta t}}{\theta(\alpha^2 + \theta^2)} d\theta = \frac{i\pi}{\alpha^2} (e^{\alpha t} - 1), \quad t < 0,$$

$$\int_{-\infty}^{\infty} \frac{e^{i\theta t}}{\alpha^2 + \theta^2 + i\beta\theta} d\theta = \frac{\pi}{\alpha_1} e^{-n_1 t}, \quad t > 0,$$

$$\int_{-\infty}^{\infty} \frac{e^{i\theta t}}{\theta(\alpha^2 + \theta^2 + i\beta\theta)} d\theta = i\pi \left[\frac{1}{\alpha^2} - \frac{e^{-n_1 t}}{\alpha_1 n_1} \right], \quad t > 0,$$

$$\int_{-\infty}^{\infty} \frac{e^{i\theta(t-h)}}{\alpha^2 + \theta^2 + i\beta\theta} d\theta = \frac{\pi}{\alpha_1} e^{n_2(h-t)}, \quad t < h,$$

$$\int_{-\infty}^{\infty} \frac{e^{i\theta(t-h)}}{\theta(\alpha^2 + \theta^2 + i\beta\theta)} d\theta = -i\pi \left[\frac{e^{n_2(h-t)}}{\alpha_1 n_2} + \frac{1}{\alpha^2} \right], \quad t < h,$$

$$\int_{-\infty}^{\infty} \frac{e^{i\theta(t-y)}}{\alpha^2 + \theta^2} d\theta = \frac{\pi}{\alpha} e^{-\alpha(t-y)}, \quad t > h,$$

$$\int_{-\infty}^{\infty} \frac{e^{i\theta(t-h)}}{\theta(\alpha^2 + \theta^2)} d\theta = i\pi \left[\frac{1}{\alpha^2} - \frac{e^{-\alpha(t-h)}}{\alpha^2} \right], \quad t > h. \quad (\text{A5})$$

Thus, by also using (24b,c), equations (A1-4) may easily be shown to reduce to

$$R_1(\alpha) = -\frac{\alpha}{2\alpha_1 n_1} \int_{a_1}^{b_1} e^{-n_1 t} \phi_1(t) dt - \frac{1}{2\alpha} \int_{a_2}^{b_2} e^{\alpha t} \phi_2(t) dt,$$

$$R_2(\alpha) = -\frac{\alpha}{2\alpha_1} \int_{a_1}^{b_1} e^{-n_1 t} \phi_1(t) dt + \frac{1}{2} \int_{a_2}^{b_2} e^{\alpha t} \phi_2(t) dt,$$

$$R_3(\alpha) = -\frac{\alpha}{2\alpha_1 n_2} \int_{a_1}^{b_1} e^{n_2(h-t)} \phi_1(t) dt + \frac{1}{2\alpha} \int_{a_3}^{b_3} e^{-\alpha(t-y)} \phi_3(t) dt,$$

$$R_4(\alpha) = -\frac{\alpha}{2\alpha_1} \int_{a_1}^{b_1} e^{n_2(h-t)} \phi_1(t) dt + \frac{1}{2} \int_{a_3}^{b_3} e^{-\alpha(t-h)} \phi_3(t) dt. \quad (\text{A6a-d})$$

APPENDIX B

Expressions of the kernels k_{ij} , ($i,j=1,2,3$) that appear in (34)

To examine the asymptotic behavior of the kernels defined by (32) and (33) we observe that for $|\alpha| \rightarrow \infty$

$$m_1 = -|\alpha| \sqrt{1 + \frac{i\beta}{\alpha}} \rightarrow -|\alpha|, \quad \alpha_1 = \alpha [1 + (\frac{\beta}{2\alpha})^2]^{1/2} \rightarrow \alpha,$$

$$n_1 \rightarrow \alpha - \frac{\beta}{2}, \quad n_2 \rightarrow -\alpha - \frac{\beta}{2}, \quad \Delta \rightarrow -4\alpha^2. \quad (\text{B1})$$

Thus, after separating the terms that become unbounded at $x=t$, $x=0=t$, and $x=h=t$, the kernels may be expressed as follows:

$$\lim_{y \rightarrow +0} h_{ij}(x,y,t) = \frac{\delta_{ij}}{t-x} + k_{ij}(x,t) \quad (\text{B2})$$

$$k_{11}(x,t) = -\frac{\beta}{2} \log|t-x| + h(x,t) + g(x,t), \quad (\text{B3})$$

$$\begin{aligned} h(x,t) = & -\frac{\beta}{2} [C_0 + \log A + \sum_{k=1}^{\infty} (-1)^k \frac{A^{2k}}{2k(2k)!} (t-x)^{2k}] \\ & + \int_0^{\infty} [(1 + \frac{\beta^2}{\alpha^2})^{1/4} \cos \frac{\theta}{2} - 1] \sin \alpha(t-x) d\alpha \\ & + \int_0^A (1 + \frac{\beta^2}{\alpha^2})^{1/4} \sin \frac{\theta}{2} \cos \alpha(t-x) d\alpha \\ & + \int_A^{\infty} [(1 + \frac{\beta^2}{\alpha^2})^{1/4} \sin \frac{\theta}{2} - \frac{\beta}{2\alpha}] \cos \alpha(t-x) d\alpha, \end{aligned} \quad (\text{B4})$$

$$\theta = \tan^{-1} \left(\frac{\beta}{\alpha} \right), \quad (\text{B5})$$

$$\begin{aligned}
g(x,t) = & e^{\frac{\beta}{2}(t-x)} \left\{ \int_0^\infty \frac{\alpha^2}{\alpha_1 \Delta} (\alpha - n_1)(\alpha + n_2) \left[-\frac{1}{n_1} e^{-\alpha_1(2h+t-x)} - \frac{1}{n_2} e^{-\alpha_1(2h-t+x)} \right] d\alpha \right. \\
& + \int_0^A \frac{\alpha^2 \beta}{\alpha_1 \Delta} [e^{-\alpha_1(t+x)} + e^{-\alpha_1(2h-t-x)}] d\alpha \\
& + \int_A^\infty \left[\frac{\alpha^2 \beta}{\alpha_1 \Delta} e^{-\alpha_1(t+x)} + \frac{\beta}{4\alpha} e^{-\alpha(t+x)} \right] d\alpha \\
& + \int_A^\infty \left[\frac{\alpha^2 \beta}{\alpha_1 \Delta} e^{-\alpha_1(2h-t-x)} + \frac{\beta}{4\alpha} e^{-\alpha(2h-t-x)} \right] d\alpha \\
& \left. + \frac{\beta}{4} \text{Ei}[-A(t+x)] + \frac{\beta}{4} \text{Ei}[-A(2h-t-x)] \right\}, \tag{B6}
\end{aligned}$$

$$\begin{aligned}
K_{12}(x,t) = & \frac{1}{t-x} + \int_0^A \left\{ \frac{2\alpha}{\Delta} [-(\alpha + n_2) e^{-2\alpha_1 h} e^{\alpha t} e^{n_1 x} + (\alpha + n_1) e^{\alpha t} e^{n_2 x}] + e^{-\alpha(x-t)} \right\} d\alpha \\
& + \int_A^\infty \left\{ \frac{2\alpha}{\Delta} [-(\alpha + n_2) e^{-2\alpha_1 h} e^{\alpha t} e^{n_1 x} + (\alpha + n_1) e^{\alpha t} e^{n_2 x}] + e^{-\alpha(x-t)} - \frac{\beta}{4\alpha} e^{-\alpha(x-t)} \right\} d\alpha \\
& - \frac{\beta}{4} \text{Ei}[-A(x-t)], \tag{B7}
\end{aligned}$$

$$\begin{aligned}
K_{13}(x,t) = & \frac{1}{t-x} + \int_0^A \left\{ \frac{2\alpha}{\Delta} [-(\alpha - n_2) e^{n_1(h-x)} e^{-\alpha(t-h)} + (\alpha - n_1) e^{-2\alpha_1 h} e^{-\alpha(t-h)} e^{n_2(h-x)}] \right. \\
& \left. - e^{-\alpha(t-x)} \right\} d\alpha + \int_A^\infty \left\{ \frac{2\alpha}{\Delta} [-(\alpha - n_2) e^{-n_1(h-x)} e^{-\alpha(t-h)} \right. \\
& \left. + (\alpha - n_1) e^{-2\alpha_1 h} e^{-\alpha(t-h)} e^{-n_2(h-x)} \right] - e^{-\alpha(t-x)} - \frac{\beta}{4\alpha} e^{-\alpha(t-x)} \right\} d\alpha \\
& - \frac{\beta}{4} \text{Ei}[-A(t-x)], \tag{B8}
\end{aligned}$$

$$\begin{aligned}
K_{21}(x,t) &= \frac{1}{t-x} + \int_0^A \left\{ \frac{2\alpha^2}{\Delta} \left[-\frac{(\alpha+n_1)}{n_1} e^{-n_1 t} e^{\alpha x} + \frac{(\alpha+n_2)}{n_2} e^{-n_1 h} e^{n_2(h-t)} e^{\alpha x} \right] e^{-\alpha(t-x)} \right\} d\alpha \\
&+ \int_A^\infty \left\{ \frac{2\alpha^2}{\Delta} \left[-\frac{(\alpha+n_1)}{n_1} e^{-n_1 t} e^{\alpha x} + \frac{(\alpha+n_2)}{n_2} e^{-n_1 h} e^{n_2(h-t)} e^{\alpha x} \right] e^{-\alpha(t-x)} \right. \\
&\left. - \frac{\beta}{4\alpha} e^{-\alpha(t-x)} \right\} d\alpha - \frac{\beta}{4} \text{Ei}[-A(t-x)] , \tag{B9}
\end{aligned}$$

$$\begin{aligned}
K_{22}(x,t) &= \int_0^A \left[-\frac{\alpha\beta}{\Delta} (1-e^{-2\alpha_1 h}) \right] e^{\alpha(t+x)} d\alpha \\
&+ \int_A^\infty \left[-\frac{\alpha\beta}{\Delta} (1-e^{-2\alpha_1 h}) - \frac{\beta}{4\alpha} \right] e^{\alpha(t+x)} d\alpha \\
&- \frac{\beta}{4} \text{Ei}[-A(t+x)] , \tag{B10}
\end{aligned}$$

$$\begin{aligned}
K_{31}(x,t) &= \frac{1}{t-x} + \int_0^\infty \left\{ \frac{2\alpha^2}{\Delta} \left[\frac{(\alpha-n_1)}{n_1} e^{n_2 h} e^{-n_1 t} e^{-\alpha(x-h)} - \frac{(\alpha-n_2)}{n_2} e^{n_2(h-t)} e^{-\alpha(x-h)} \right] \right. \\
&\left. + e^{-\alpha(x-t)} \right\} d\alpha + \int_0^\infty \left\{ \frac{2\alpha^2}{\Delta} \left[\frac{(\alpha-n_1)}{n_1} e^{n_2 h} e^{-n_1 t} e^{-\alpha(x-h)} \right. \right. \\
&\left. \left. - \frac{(\alpha-n_2)}{n_2} e^{n_2(h-t)} e^{-\alpha(x-h)} \right] + e^{-\alpha(x-t)} - \frac{\beta}{4\alpha} e^{-\alpha(x-t)} \right\} d\alpha \\
&- \frac{\beta}{4} \text{Ei}[-A(x-t)] , \tag{B11}
\end{aligned}$$

$$\begin{aligned}
K_{33}(x,t) &= \int_0^A \left[-\frac{\alpha\beta}{\Delta} (1-e^{-2\alpha_1 h}) \right] e^{-\alpha(t+x-2h)} d\alpha \\
&+ \int_A^\infty \left[-\frac{\alpha\beta}{\Delta} (1-e^{-2\alpha_1 h}) - \frac{\beta}{4\alpha} \right] e^{-\alpha(t+x-2h)} d\alpha \\
&- \frac{\beta}{4} \text{Ei}[-A(t+x-2h)]
\end{aligned} \tag{B12}$$

In equations (B4-B12), $C_0=0.5772156649$ is the Euler's constant, A is any positive constant and the Exponential Integral $\text{Ei}[-Az]$ is defined by ($A>0, z>0$)

$$\begin{aligned}
\text{Ei}[-Az] &= - \int_A^\infty \frac{1}{\alpha} e^{-\alpha z} d\alpha \\
&= C_0 + \log A + \log z + \int_0^{Az} \frac{e^{-\alpha} - 1}{\alpha} d\alpha \\
&= C_0 + \log A + \log z + \sum_{k=1}^{\infty} \frac{(-1)^k A^k z^k}{k(k!)}
\end{aligned} \tag{B13}$$

where rapid convergence is insured by selecting $0 < A < 1$.